Abstract

Title of Dissertation: Signal Corrections and Calibrations of the LUX Dark Matter Detector

Richard Knoche, Doctor of Philosophy, 2016

Dissertation directed by: Professor Carter Hall,Department of Physics

Department of Physics

Abstract Blah

Signal Corrections and Calibrations of the LUX Dark Matter Detector

by

Richard Knoche

Dissertation submitted to the Faculty of the Graduate School of the
University of Maryland, College Park in partial fulllment
of the requirements for the degree of
Doctor of Philosophy
2016

Advisory Committee:
Professor Carter Hall, Chair/Adviser
Professor Person One
Professor Person Two
Professor Person Three
Professor Person Four

Acknowledgments

Acknowledgments Blah

Contents

List of Tables

List of Figures

1 Introduction to Dark Matter

In recent decades it has been discovered that the luminous matter which scientists have studied for centuries is only a small fraction of the total composition of the universe. There is strong evidence of dark baryonic matter (a few percent), non-baryonic hot dark matter (∼0.1%-1.5%), non baryonic cold dark matter (∼27%), and dark energy (∼68%) components to the universe, where the percentages are as a fraction of their total contribution to the universe's composition. While we know a large amount about the "normal" matter which contributes $\lesssim 5\%$ of the universe's total composition, we know very little about these larger components. In particular, while we understand certain characteristics of the cold dark matter component, there is no consensus on its composition. Before examining the experiments which seek to answer this question we will first discuss what is currently known about the nonbaryonic dark matter component.

1.1 Evidence for Dark Matter

1.1.1 Mass Measurements from Galactic Rotation Curves

In the early 1930's Fritz Zwicky was the first to use the Virial theorem to determine the total mass of the Coma cluster of galaxies. In his examination, Zwicky found that the velocities at large radii were too high to be consistent with the Newtonian prediction arising from the visible matter alone [32]. This discrepancy was reinforced in the 1970's, when further data on the rotational velocity of spiral galaxies began to be collected. Instead of the rotational velocity falling off as $\propto 1/\sqrt{r}$ beyond the radius of visible matter as one would expect, the rotational velocity rises for small radii, then asymptotes to a constant $v \simeq 100 - 300\ km/s$ for large radii in most galaxies [22, 12, 9]. The most widely accepted explanation of this phenomenon is that the disk galaxies are immersed in a dark matter (DM) halo such that $M(r)/r$ remains constant at large radii. Such a halo could form from an isotropic sphere of ideal gas at a uniform temperature.

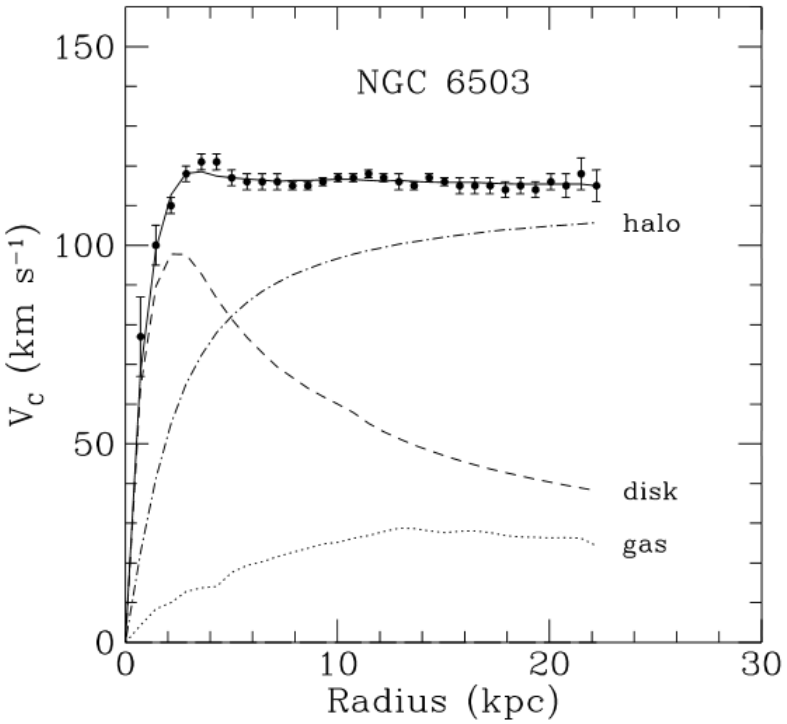

Figure 1: Rotation curve of galaxy NGC 6503. The dotted line indicates the contribution of baryonic gas, the dashed line indicates the contribution of visible matter in the disk, and the dash-dotted line indicates the contribution of dark matter. In the absence of dark matter the total velocity curve would fall off in a manner similar to the dotted line.[6]

Following Zwicky's footsteps, we can use the Virial theorem to calculate the luminous matter's contribution to the total mass of the Coma Cluster. The theorem states that for a system of N particles

$$\frac{1}{2}\sum_{i=1}^{N}\langle m_i v_i^2\rangle = -\frac{1}{2}\sum_{i=1}^{N}\langle \mathbf{r}_i \cdot \mathbf{F}_i\rangle \tag{1}$$

where m_i,v_i, and $\mathbf{r}_i$ are the mass, velocity, and position of the ith particle in a system of particles, and $\mathbf{F}_i$ is the force acting on the same particle. Since the total

force on a particle is the sum of all of the forces acting on it

$$\mathbf{F}_i = \sum_{j=1}^{N} \mathbf{F}_{ji} \tag{2}$$

where $\mathbf{F}_{ji}$ is the force that particle j applies on particle i. Noting that a particle does not apply force to itself, and that Newton's third law of motion states that $\mathbf{F}_{ji} = -\mathbf{F}_{ij}$ we can rewrite the right hand side of the Virial theorem to be

$$\sum_{i=1}^{N} \mathbf{F}_i \cdot \mathbf{r}_i = \sum_{i=1}^{N} \sum_{j<i} \mathbf{F}_{ji} \cdot \mathbf{r}_i + \sum_{i=1}^{N} \sum_{j>i} \mathbf{F}_{ji} \cdot \mathbf{r}_i = \sum_{i=1}^{N} \sum_{j<i} \mathbf{F}_{ji} \cdot (\mathbf{r}_i - \mathbf{r}_j). \tag{3}$$

Using the law of gravitation to apply equation 3 to a cluster of galaxies, the Virial theorem becomes

$$\sum_{i=1}^{N} \langle m_i v_i^2 \rangle = \sum_{i}^{N} \sum_{j<i} \left\langle \frac{G m_i m_j}{r_{ij}} \right\rangle \tag{4}$$

where G is the gravitational constant. The left hand side of this equation is the total mass, M, of the cluster of galaxies multiplied by the time and mass averaged squared velocity. The right hand side is approximately equal to $\frac{GM^2}{R}$, where R is the radius of the galaxy cluster. Rearranging equation 4, we arrive at an equation which relates the total mass of the galaxy cluster to the mean square velocity

$$M \approx \frac{\langle v^2 \rangle R}{G} \tag{5}$$

The mean square velocity of a galaxy cluster can be estimated by calculating the one dimensional line of sight velocity via redshift. Under the assumption of spherical symmetry

$$\langle v^2 \rangle = 3\langle (v_r - c\langle z \rangle)^2 \rangle \tag{6}$$

where $\langle z \rangle$ is the measured redshift of the galaxy cluster, v_r is the line of sight velocity, and c is the speed of light. For the Coma cluster $\langle z \rangle = 0.0232$, which produces an estimate of $\langle v^2 \rangle \approx 2 \times 10^{12} \frac{m^2}{s^2}$.[26] Using the measured radius of the Comma cluster ($R \approx 5 \times 10^{22}$) the total mass of the system in terms of solar mass ($M_\odot$) is found to be

$$M_{total} \approx 2 \times 10^{15} M_\odot. \tag{7}$$

Comparing this the mass calculated from luminous matter alone we see that these components contribute only a small fraction of the total mass of the system. [26]

$$\frac{M_{lum}}{M_{total}} \approx \frac{2.3 \times 10^{14} M_\odot}{2 \times 10^{15} M_\odot} = 0.11 \tag{8}$$

1.1.2 Mass Measurements from x-ray Gases

The total mass of a dynamically relaxed galaxy cluster can be measured from the hydrostatic equilibrium equation, which can be derived from the Tolman-Oppenheimer-Volkoff equation for stellar structure by taking the nonrelativistic limit of $c \to \infty$, such that

$$\frac{dP}{dr} = -\frac{GM(r)}{r^2}\rho \tag{9}$$

where P is the pressure of the gas in a cluster, G is the gravitational constant, $M(r)$ is the mass of the galaxy cluster at a particular radius, and ρ is the density of the gas in the cluster. From the ideal gas law we know that

$$P = \left(\frac{\rho}{\mu m_H}\right) kT \tag{10}$$

where μ is the mean molecular weight ($\sim$0.6 for an ionized plasma), m_H is the mass of the hydrogen atom, and k is Boltzman's constant. Plugging this into equation 9 yields

$$\frac{k}{\mu m_H}\left(T\frac{d\rho}{dr}+\rho\frac{dT}{dr}\right)=-\frac{GM(r)}{r^2}\rho \tag{11}$$

Solving equation 11 for $M(r)$ produces a measurement of the cluster's mass from x-ray gas density and temperatures

$$M(r)=-\frac{kT}{\mu m_H G}\left(\frac{d\,\ln(\rho)}{d\,\ln(r)}+\frac{d\,\ln(T)}{d\,\ln(r)}\right)r \tag{12}$$

where the logarithms were introduced using the fact that

$$\frac{r}{t}\frac{dT}{dr}=\frac{\frac{dT}{T}}{\frac{dr}{r}}=\frac{d\,\ln T}{d\,\ln r}. \tag{13}$$

This mass measurement technique is complicated by the fact that the gas density and temperature of a galaxy cluster has spatial variation, as well as the fact that x-ray emission measurements are a two-dimensional projection of a three-dimensional object, which produces complications when integrating x-ray spectra along lines of sight through the cluster. One method for simplifying the mass measurement, called the beta model, is to assume the cluster is made of isothermal, spherically symmetric gas. In this case the density of the gas traces the density of the gravitational mass, such that

$$\rho_{gas}(r)=\rho_0\left(1+\frac{r}{r_c}\right)^{-3\beta/2} \tag{14}$$

where r_c is the core radius, ρ_0 is the central density, and β is a slope parameter. [30] The core radius r_c is defined using the intensity of x-ray observations such that $I(r_c) = \frac{1}{2}I(0)$, or more generally to be the radius at which $\frac{d^2 \ln(I)}{d \ln(r)^2}$ is maximized. In this model the mass measurement reduces to a derivation of the spatial density profile by determining the best fit parameters of r_c and β to the x-ray observations. When this mass measurement technique is compared to mass measurements from luminous matter alone more evidence for dark matter arises. For example, using this technique the Virgo Cluster has been measured to have a total mass (within r < 1.8Mpc) between $1.5 \times 10^{14} M_\odot$ and $5.5 \times 10^{14} M_\odot$. [29] Comparing this to the mass measured from x-ray luminosity yields a ratio of

$$\frac{M_{lum}}{M_{total}} \approx \frac{4.75 \times 10^{13} M_\odot}{3.5 \times 10^{14} M_\odot} = 0.14 \tag{15}$$

1.1.3 Gravitational Lensing

Gravitational lensing provides an independent method for measuring the mass of galaxy clusters and other astronomical objects. Gravitational lensing can be divided into two categories – strong lensing and weak lensing. Strong lensing, in which a background light source is distorted into arcs around a massive foreground object, is a rare phenomenon which requires a light source and a very massive lens to be nearly in line with the observer. When such a situation occurs the mass of the lens can be inferred from the angular width of the arc of light which is produced. We turn to general relativity to derive the equation which produces this mass measurement.

The geodesic equation, which describes the path that a free particle travels, is

given by

$$\frac{d}{d\tau}\left(g_{aj}\frac{dx^j}{d\tau}\right) - \frac{1}{2}\frac{\partial g_{ij}}{\partial x^a}\frac{dx^i}{d\tau}\frac{dx^j}{d\tau} = 0 \tag{16}$$

where $g_{\alpha j}$ is a metric, τ is the proper time, and x is the four dimensional coordinate vector. For a spacetime in a vacuum outside of a spherically symmetric mass the appropriate metric to use is the Schwarzschild metric. With units of $c = 1$ it is given by

$$ds^2 = -\left(1 - \frac{2GM}{r}\right)dt^2 + \left(1 - \frac{2GM}{r}\right)^{-1}dr^2 + r^2 d\theta^2 + r^2 sin^2\theta d\phi^2. \tag{17}$$

From the t component of the geodesic equation we know that

$$\frac{d}{d\tau}\left(g_{tj}\frac{dx^j}{d\tau}\right) - \frac{1}{2}\frac{\partial g_{ij}}{\partial t}\frac{dx^i}{d\tau}\frac{dx^j}{d\tau} = 0. \tag{18}$$

The Schwarzschild metric does not depend on time, and is diagonal, therefore

$$\frac{d}{d\tau}\left(g_{tj}\frac{dx^j}{d\tau}\right) = \frac{d}{d\tau}\left(g_{tt}\frac{dt}{d\tau}\right) = -\frac{d}{d\tau}\left(\left(1 - \frac{2GM}{r}\right)\frac{dt}{d\tau}\right) = 0. \tag{19}$$

Equation 18 is true if the quantity inside of the derivative is constant, leading us to the first constant of motion

$$E = \left(1 - \frac{2GM}{r}\right)\frac{dt}{d\tau}. \tag{20}$$

We now turn to the ϕ component of the geodesic equation

$$\frac{d}{d\tau}\left(g_{\phi j}\frac{dx^j}{d\tau}\right) = \frac{d}{d\tau}\left(g_{\phi\phi}\frac{d\phi}{d\tau}\right) = -\frac{d}{d\tau}\left(r^2 sin^2\theta\frac{d\phi}{d\tau}\right) = 0 \tag{21}$$

where we have once again used the fact that the metric does not depend on time and is diagonal to simplify the equation. From this we arrive at the second constant of motion

$$l = r^2 sin^2\theta \frac{d\phi}{d\tau} \tag{22}$$

Returning to the Schwarzschild metric, for a photon ds^2=0, and if we assume motion in the equatorial plane $\theta = \pi/2$ and $d\theta = 0$, such that

$$-\left(1 - \frac{2GM}{r}\right) dt^2 + \left(1 - \frac{2GM}{r}\right)^{-1} dr^2 + r^2 d\phi^2 = 0. \tag{23}$$

From the two constants of motion we know that

$$d\phi^2 = \frac{l^2}{r^4 sin^4\theta} d\tau^2 \tag{24}$$

and

$$dt^2 = E^2 \left(1 - \frac{2GM}{r}\right)^{-2} d\tau^2 \tag{25}$$

Plugging equations 24 and 25 into equation 23 and simplifying yields

$$dr^2 = \left[E^2 - \left(1 - \frac{2GM}{r}\right) \frac{l^2}{r^2}\right] d\tau^2 \tag{26}$$

Finally, by dividing equation 26 by 24 we arrive at the equation of motion for light traveling in a Schwarzschild spacetime in polar coordinates

$$\left(\frac{1}{r^2}\frac{dr}{d\phi}\right)^2 = \left(\frac{E}{l}\right)^2 - \left(1 - \frac{2GM}{r}\right)\frac{1}{r^2} \equiv \left(\frac{1}{b}\right)^2 - \left(1 - \frac{2GM}{r}\right)\frac{1}{r^2} \tag{27}$$

The quantity $b \equiv l/E$ is known as the impact parameter, which represents the

perpendicular distance between the center of attraction and the particle's initial trajectory. To determine the change in the direction of light due to a gravitational field we must integrate $\frac{d\phi}{dr}dr$ from the minimum distance the light travels by the massive object, denoted as R, and then multiply by a factor of 2 to account for the symmetrical motion of the particle during its approach to the object. Note that at a distance R the light is moving tagentially, such that $\frac{dr}{dt} = 0$ and equation 27 becomes

$$\frac{1}{b^2} = \left(1 - \frac{2GM}{R}\right)\frac{1}{R^2}. \tag{28}$$

Therefore, we can rewrite equation 27 for any value of r as

$$\left(\frac{1}{r^2}\frac{dr}{d\phi}\right)^2 = \left(1 - \frac{2GM}{R}\right)\frac{1}{R^2} - \left(1 - \frac{2GM}{r}\right)\frac{1}{r^2}. \tag{29}$$

Making the convenient substitution of $u \equiv R/r$, where $0 \leq u \leq 1$ in equation 29 yields

$$\left(\frac{du}{d\phi}\right)^2 = 1 - u^2 - \frac{2GM}{r}(1 - u^3). \tag{30}$$

From this we can find an equation for the infinitesimal variation $d\phi$ in terms of du

$$d\phi = \frac{(1-u^2)^{-1/2}du}{\left[1 - \frac{2GM}{R}(1-u^3)(1-u^2)^{-1}\right]^{-1/2}}. \tag{31}$$

A further substitution of $u \equiv \cos(\alpha)$, where $0 \leq \alpha \leq \pi/2$, leads (after some simplification) to the equation

$$d\phi = \left[1 - \frac{2GM}{R}\left(\cos(\alpha) + \frac{1}{1+\cos(\alpha)}\right)\right]^{-1/2} d\alpha. \tag{32}$$

In most cases, the quantity $M/R << 1$, so we can use the approximation $(1+x)^n \approx 1+nx$ for small x in equation 32 such that

$$d\phi = \left[1 + \frac{GM}{R}\left(\cos(\alpha) + \frac{1}{1+\cos(\alpha)}\right)\right] d\alpha. \tag{33}$$

This is known as the "weak field" limit. Integrating this expression from $0 \leq \alpha \leq \pi/2$ and multiplying by 2 to account for the two symmetrical legs of the light's trajectory provides an expression for the total azimuthal angle of the light.

$$\phi = 2\int_0^{\pi/2} \left[1 + \frac{GM}{R}\left(\cos(\alpha) + \frac{1}{1+\cos(\alpha)}\right)\right] d\alpha = \pi + \frac{4GM}{R}. \tag{34}$$

Noting that the first term, π, is the azimuthal angle of the light if no mass were present, we arrive at an equation that relates the angle of deflection of light to the total mass of the gravitational object.

$$\Delta\phi = \phi - \pi = \frac{4GM}{R}. \tag{35}$$

In practice, we must go one step further to turn astronomical observations of gravitational lensing into a mass measurement. Any observation of a lensed light source involves an observer viewing an image of the object after it passes by a gravitational lens. This situation is depicted in Figure 2. To measure the mass of a lens we seek to relate the source position to the image position. Using the small angle approximation for θ and β we can arrive at

$$D_S\theta = D_S\beta + D_{LS}\Delta\phi. \tag{36}$$

where $D_s = D_L + D_{LS}$ is the distance from the source plane to the observer. Using equation 35, and the fact that $R \approx \theta D_L$ this becomes

$$\theta = \beta + \frac{4GMD_{LS}}{\theta D_L D_S} \tag{37}$$

This is a quadratic equation with roots

$$\theta = \frac{\beta \pm \sqrt{\beta^2 + 4\theta_E^2}}{2} \tag{38}$$

where $\theta_E = \left(4GM\frac{D_{LS}}{D_S D_L}\right)^{1/2}$ is the angular size of the "Einstein ring" that forms when the source and lens are perfectly aligned. If the quantities D_{LS}, D_L, and β are known, equation 38 can be used to measuring the mass of the lens by measure the angle of deflection θ. [8] In the handful of cases in which this mass measurement has been carried out, it has been found to be consistent with dark matter models. [31]

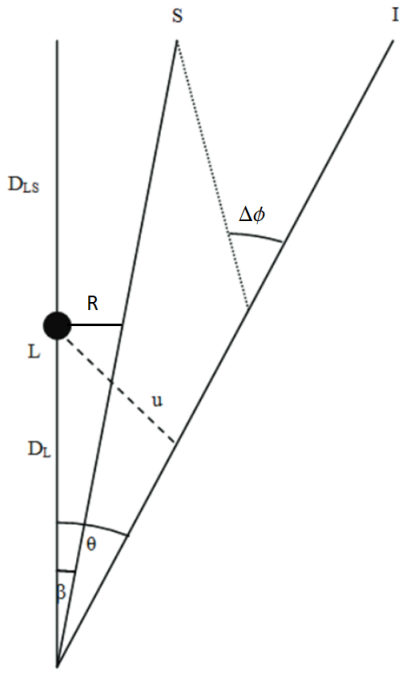

Figure 2: A source emits light at position S. The light is deflected by a massive lens at L, and causes the image seen by the observer to appear at an angle θ. D_{LS}, D_L, θ, and β are, respectively, the distance from the lens plane to the source plane, the distance from the lens plane to the observer, the angle of the image relative to the observer, and the angle of the source relative to the observer. [8]

Although there are only a few cases in which strong gravitational lensing can be observed, there are numerous cases of weak gravitational lensing. Weak lensing occurs when the lensing mass isn't large enough for strong lensing, or if the source of light is not directly aligned with the lensing mass, resulting in a shear distortion of the image. Measuring the mass of a weak lens is complicated by the fact that each light source has a unique, intrinsic ellipticity which typically dwarfs the magnitude of the image distortion. This intrinsic ellipticity is known as "shape noise" in weak gravitational lensing studies. In cases where many sources are lensed by the same object, the distortion from the lens can be measured by averaging over the many source images, taking advantage of their random intrinsic orientation.

In these cases, the measured shear distortion results from photons being deflected by mass fluctuations along the line of sight. In this case, the two dimensional lens equation (analogous to equation 37) in vector format is

$$\boldsymbol{\beta} = \boldsymbol{\theta} - \frac{D_{LS}}{D_S}\Delta\boldsymbol{\phi}(\boldsymbol{\xi}) \tag{39}$$

where $\boldsymbol{\xi} = D_S\boldsymbol{\theta}$ is the impact parameter. The deflection angle can be calculated by integrating the 3D gravitational potential, $\boldsymbol{\Phi}(\mathbf{r})$, along the line of sight such that

$$\Delta\boldsymbol{\phi}(\boldsymbol{\xi}) = 2\int \nabla_\perp \boldsymbol{\Phi}(\mathbf{r})dz = \nabla_\perp\left(2\int \boldsymbol{\Phi}(\mathbf{r})dz\right) \equiv \nabla_\perp V. \tag{40}$$

Assuming the angle between the image and the observer, $\boldsymbol{\theta}$, is small equation 39 can be approximated with a first order Taylor series as

$$\beta_i = A_{ij}\theta_j \tag{41}$$

where i corresponds to the i^{th} component of the lens plane, j corresponds to the j^{th} component of the source plane, and

$$A_{ij} = \frac{\partial\beta_i}{\partial\theta_j} = \delta_{ij} - \frac{\partial\Delta\phi_i(\boldsymbol{\theta})}{\partial\theta_j} = \delta_{ij} - \frac{\partial^2 V(\boldsymbol{\theta})}{\partial\theta_i\partial\theta_j} \tag{42}$$

are the elements of a Jacobian distortion matrix, $\mathbf{A}$, which describes the isotropic dilation and anisotropic distortion due to convergence and shear effects. The distortion matrix can be written in terms of the convergence, κ, which increases the size of the image while conserving brightness, and the shear, γ, which distorts

the the image tangentially around the lens.

$$A_{ij} = (1-\kappa)\begin{pmatrix} 1 & 0 \\ 0 & 1 \end{pmatrix} - \gamma \begin{pmatrix} \cos(2\phi) & \sin(2\phi) \\ \sin(2\phi) & -\cos(2\phi) \end{pmatrix} \tag{43}$$

Equations 42 and 43 offer a relationship between the observable quantities κ and γ, and the gravitational potential V.

$$\gamma_1 \equiv \gamma cos2\phi = \frac{1}{2}\left[\frac{\partial^2 V(\boldsymbol{\theta})}{\partial\theta_1^2} - \frac{\partial^2 V(\boldsymbol{\theta})}{\partial\theta_2^2}\right] \tag{44}$$

$$\gamma_2 \equiv \gamma \sin(2\phi) = \frac{\partial^2 V(\boldsymbol{\theta})}{\partial\theta_1\partial\theta_2} \tag{45}$$

$$\kappa = \frac{1}{2}\nabla^2 V(\boldsymbol{\theta}) \tag{46}$$

where equation 44 comes from $A_{11} - A_{22}$, equation 45 comes from $A_{12} - A_{21}$, and equation 46 comes from $tr(A)$. Since κ is equal to half the laplacian of the projected gravitational potential, V, it is directly proportional to the mass density of the lens. The shear component γ_1 corresponds to elongation and compression along the x and y directions, and the component γ_2 describes elongation and compression along the diagonal $x = y$ and $x = -y$ directions. In the case of weak lensing, the mass measurement then reduces to a measurement of the shear and convergence produced by the lens. [23]. As with strong gravitational lensing, weak gravitational lensing mass measurements have been found to be consistent with dark matter models. [31]

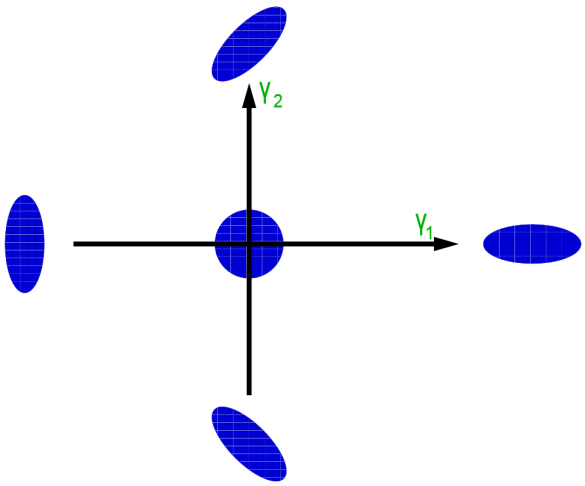

Figure 3: An illustration of how positive and negative γ_1 and γ_2 distort an object with initial ellipticity of zero. [24]

One of the most famous instances of weak lensing evidence for dark matter is a collision of two galaxies clusters known as the Bullet Cluster. The baryonic matter in each galaxy cluster is predominantly in the form of hot gas. Electromagnetic interaction causes the gas to to slow down and concentrate in the center of the collision. In the absence of dark matter gravitational lensing measurements should be correlated with the hot gas, since it is the dominant luminous mass in the system. However, if dark matter was a dominant mass component in the Bullet Cluster it would not be slowed by electromagnetic interactions and would pass through the collision without significant perturbation. Indeed, weak gravitational lensing observations show that the majority of the mass in the Bullet Cluster passed through the collision rather than concentrating at the center like the luminous matter, suggesting that dark matter is present in abundance over the baryonic matter of the two galaxy clusters. [11]

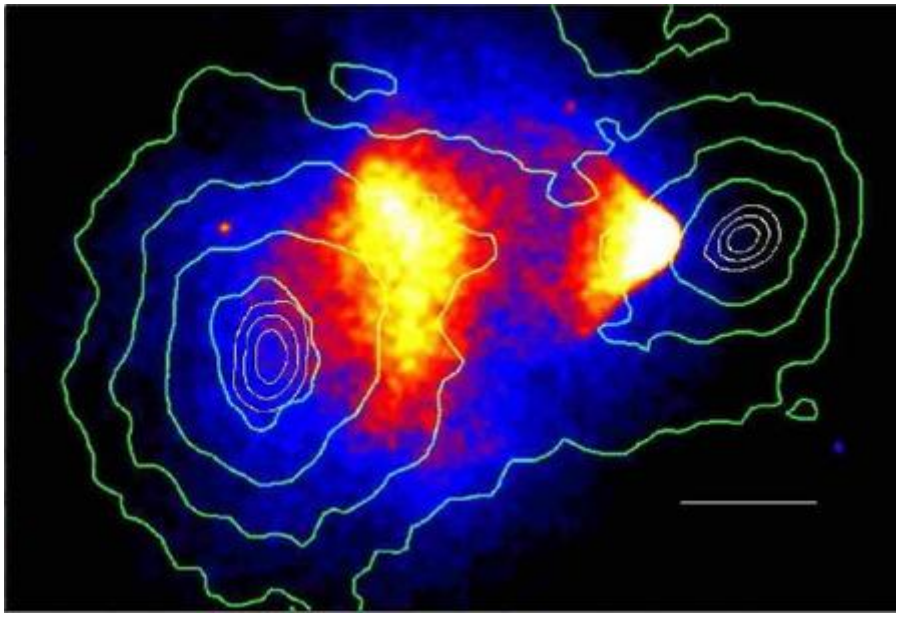

Figure 4: X-ray image of the baryonic mass in the Bullet cluster, overlayed with mass contours derived from weak lensing measurements. The separation of the dominant mass component from the baryonic matter indicates the presence of dark matter. [11]

1.1.4 Cosmological Evidence

The early universe was filled with a hot, dense plasma of electrons and baryons. At this time photons scattered off of the free electrons, restricting their movement across the universe. As the universe cooled below the binding energy of hydrogen (13.6 eV) protons and electrons began to combine, forming neutral hydrogen atoms. At this point in time, known as the recombination epoch, photons and electrons decoupled and the photons began traveling with a mean free path the size of the universe. These photons produce the Cosmic Microwave Background (CMB) that we see today. (Figure 5) The radiation is extremely isotropic and exhibits a black-body spectrum at a red shifted temperature of 2.72 K. The frequency spectrum, temperature fluctuations, and polarization of the CMB all contain a vast amount

of information about the formation of the universe. Here, we focus on just one of these properties.

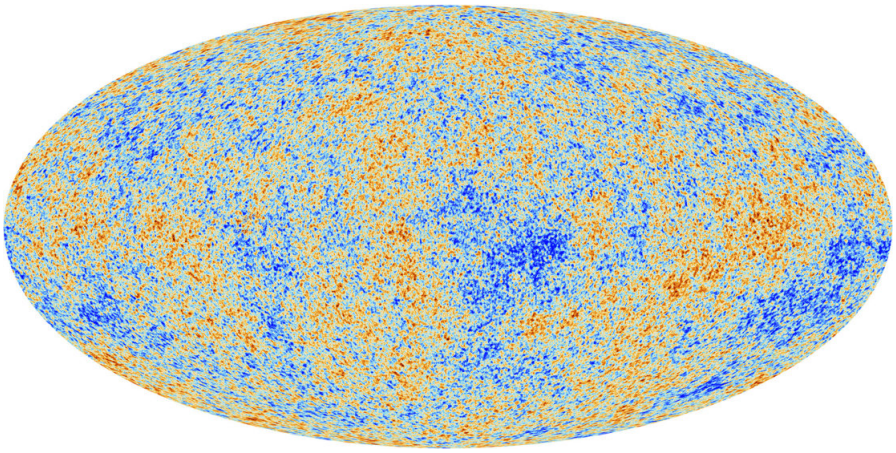

Figure 5: The latest measurement of the CMB temperature anistropies from Planck data. [1]

In 2003 the WMAP satellite observed small (1 part in 10,000) fluctuations in the average temperature of the CMB. We see these temperature fluctuations projected on a 2D spherical surface, so it is typical to expand them in terms of spherical harmonics defined by

$$Y_{lm} = \sqrt{\frac{2l+1}{4\pi}\frac{(l-m)!}{(l+m)!}} P_l^m(\cos\theta) e^{im\phi} \tag{47}$$

where $l = 0, ..., \infty$, $-l \leq m \leq l$, and P_l^m are associated Legendre polynomials. The temperature fluctuations can then be written as

$$f(\theta,\phi) \equiv \frac{\delta T(\theta,\phi)}{T_0} = \sum_{l=0}^{l=\infty} \sum_{m=-l}^{m=l} a_{lm} Y_{lm}(\theta,\phi) \tag{48}$$

where T_0 is the average temperature of the CMB and a_{lm} are the coefficients of expansion. Since the spherical harmonics are orthonormal

$$a_{lm} = \int_{\theta=-\pi}^{\pi} \int_{\phi=0}^{2\pi} f(\theta,\phi) Y^*_{lm}(\theta,\phi) d\Omega \tag{49}$$

and since a_{lm} are independent random variables

$$\langle a_{lm} a^*_{l'm'} \rangle = \delta_{ll'} \delta m m' \left\langle |a_{lm}|^2 \right\rangle . \tag{50}$$

The temperature fluctuations are isotropic and therefore independent of m, so

$$\left\langle |a_{lm}|^2 \right\rangle = \frac{1}{2l+1} \sum_m \left\langle |a^2_{lm}| \right\rangle \equiv C_l. \tag{51}$$

where the function C_l is referred to as the angular power spectrum of the temperature fluctuations. The angular power spectrum is related to contribution of the multipole l to the temperature variance by

$$\begin{aligned} \left\langle \left(\frac{\delta T(\theta,\phi)}{T_0} \right)^2 \right\rangle &= \left\langle \sum_{lm} a_{lm} Y_{lm}(\theta,\phi) \sum_{l'm'} a^*_{l'm'} Y^*_{l'm'}(\theta,\phi) \right\rangle \\ &= \sum_{ll'} \sum_{mm'} Y_{lm}(\theta,\phi) Y^*_{l'm'}(\theta,\phi) \left\langle a_{lm} a^*_{l'm'} \right\rangle \\ &= \sum_l C_l \sum_m |Y_{lm}(\theta,\phi)|^2 = \sum_l \frac{2l+1}{4\pi} C_l \end{aligned} \tag{52}$$

where we have used the the closure relation

$$\sum_m |Y_{lm}(\theta,\phi)|^2 = \frac{2l+1}{4\pi} \tag{53}$$

in the last step of equation 52. [19]

Cosmological models predict the variance of the a_{lm} expansion coefficients, and therefore predict the angular power spectrum and the contribution of each multipole to the temperature variance. By measuring the angular power spectrum of the CMB and comparing to the C_l values predicted by each model we can learn about the composition of the universe. The temperature fluctuations of the CMB are typically plotted in terms of $D_l \equiv l(l+1)C_l/(2\pi)$ with units of μK^2 versus the multipoles l as shown in Figure 6.

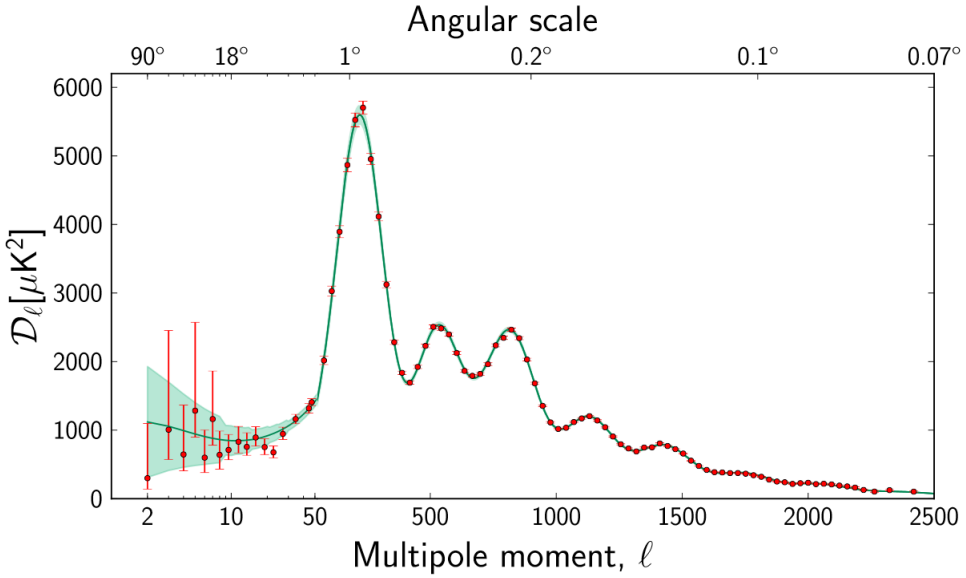

Figure 6: The power spectrum of temperature fluctuations from the CMB based on data from Planck. [1]

To understand the wealth of information present in Figure 6 we must first understand the origin of the temperature fluctuations in the early universe. Prior to recombination the primordial plasma consisted of anistropic regions of varying density. Overdense regions of matter would gravitationally attract more matter. As this happened, heat from photons scattering off of free electrons would produce

an increase in pressure, counteracting the force of gravity and pushing baryonic matter away from the high density regions. As these two processes competed they produced oscillations in the distribution of baryonic matter, which we refer to as Baryon acoustic oscillations (BAO). After recombination the photons diffused through the baryonic matter, removing the source of pressure, ending the oscillating process, and leaving a shell of overdense baryonic matter at the origin of the anisotropy and at a fixed radius called the sound horizon.

The first peak in Figure 6 details the curvature of the universe. If the universe had positive curvature the light from the CMB would be magnified, shifting the first peak to lower multipole in Figure 6. Likewise, in a negatively curved universe the scale of the temperature fluctuations in the CMB would appear diminished, shifting the first peak to higher multipole. The observed location of the first peak, close to $l \sim 200$, turns out to be consistent with a flat universe.

The second peak in Figure 6 details the amount of baryonic matter in the universe. Baryons add mass to the system during the oscillating process described above. This additonal inertia forces the primordial plasma to travel farther before recoiling back to the center of the anistropy, much like adding a mass to the end of a spring. The odd numbered peaks in Figure 6 are associated with how far the plasma compresses during BAO and are enhanced by the presence of additional baryons, as shown in Figure 7. The even numbered peaks are associated with how far the plasma rebounds during BAO and are unaffected by the presence of additional baryons. Therefore, the presence of baryons enhances the size of the odd peaks over the even peaks such that a smaller second peak in Figure 6 corresponds to a larger amount of baryonic matter in the universe. The latest results from Planck indicate that baryonic matter makes up 4.9% of the universe.

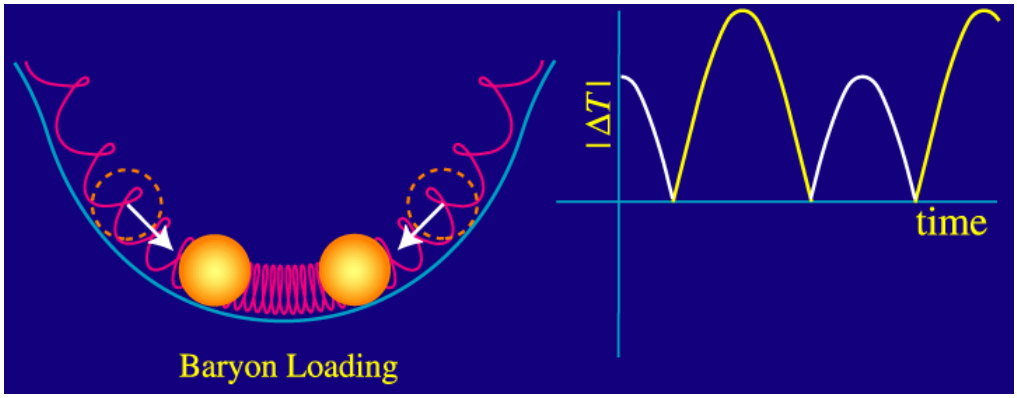

Figure 7: A depiction of the effect of baryons on the oscillating plasma during BAO. The mass of the baryons loads down the plasma, producing an asymmetry in the oscillations in which the plasma compresses further toward the minimum of the potential well. Since the CMB power spectrum does not care about the sign of the fluctuation, we see that the odd numbered peaks become enhanced over the even numbered peaks. [15]

The third peak in Figure 6 details the amount of dark matter in the universe. Since the very early universe was dominated by photon-baryon interactions, the outward pressure caused the gravitational potential of the BAO system to decay in such a way that it drove the amplitude of oscillations higher. With higher dark matter density this driving effect is diminished and the overall magnitude of the peaks becomes smaller. Although this effects all of the peaks in Figure 6 it is only distinguishable in the third peak. Furthermore, as with ordinary matter, dark matter was gravitational attracted to areas with higher density. Since dark matter does not interact through the electromagnetic force it was unaffected by the increasing photon pressure which produced acoustic oscillations in baryons. As a result, a higher density of dark matter corresponded to a larger gravitational potential well for baryons to fall into during their oscillations, increasing the amplification of BAO on the odd numbered peaks. Therefore, the height of the third peak tells us the amount of dark matter that is present in the universe. [15] The

Planck observations indicates that dark matter makes up 26.8% of the universe. The remaining 68.3% of the universe is made up of dark energy. [1]

1.2 Dark Matter Candidates

1.2.1 The ΛCDM Model

To further examine the properties of dark matter it is useful to introduce a quantitative measure for the composition of the universe. Friedmann's equation, which describes the expansion of space in a homogeneous and isotropic universe, is given by

$$\frac{\dot{a}^2 + kc^2}{a^2} = \frac{8\pi G\rho + \Lambda c^2}{3}, \tag{54}$$

where a is the scale factor of the universe, k is the spatial curvature of the universe (equivalent to one sixth of the Ricci Scalar) , c is the speed of light, G is the gravitational constant, ρ is the density of the universe, and Λ is the cosmological constant. Einstein's field equations,

$$G_{\mu\nu} = \frac{8\pi G}{c^4} T_{\mu\nu} \tag{55}$$

provide an expression for the cosmological constant, Λ. We can split the stress energy tensor into two terms, one describing matter and the other describing the vacuum, such that $T_{\mu\nu} = T^{matter}_{\mu\nu} + T^{vac}_{\mu\nu}$. Since the stress energy tensor is given by

$$T_{\mu\nu} = (\rho + p)U_\mu U_\nu + p g_{\mu\nu}, \tag{56}$$

and to maintain Lorentz invariance $p^{vac} = -\rho^{vac}$, we can write the vacuum component of the stress energy tensor as

$$T_{\mu\nu}^{vac} = -\rho^{vac} g_{\mu\nu}. \tag{57}$$

If we identify the vacuum energy density as

$$\rho^{vac} = \frac{\Lambda c^2}{8\pi G} \tag{58}$$

then Einstein's field equation takes on the familiar form

$$G_{\mu\nu} + g_{\mu\nu}\Lambda = \frac{8\pi G}{c^4} T_{\mu\nu}^{matter}, \tag{59}$$

where $G_{\mu\nu}$ is the Einstein tensor, $g_{\mu\nu}$ is the metric tensor, G is the gravitational constant, and Λ is the cosmological constant. Setting the normalized spatial curvature $k = 0$ in Friedmann's equation(representing a flat universe), one can find the critical density for which the universe is spatially flat to be

$$\rho_c = \frac{3}{8\pi G}\frac{\dot{a}^2}{a^2}, \tag{60}$$

where $\rho_c = \rho^{vac} + \rho$. Recognizing Hubble's constant to be $H = \frac{\dot{a}}{a}$, we can rewrite this as

$$\rho_c = \frac{3H^2}{8\pi G} \tag{61}$$

where H is the present value of the Hubble constant [16]. The current experimental value for H in the dimensionless units 100 km/s/Mpc is $h \sim 0.7$ with an uncertainty

of $\sim 5\%$. We can then define the density parameter as

$$\Omega = \frac{\rho}{\rho_c} = \frac{8\pi G\rho}{3H_0^2}. \tag{62}$$

If Ω is larger than unity the universe is spatially closed, and if Ω is less than unity the universe is spatially open. This density parameter can be split into components, such that for a particular component x

$$\Omega_x = \frac{\rho_x}{\rho_c}. \tag{63}$$

Detailed cosmological studies have concluded that all the luminous matter in the universe has a density parameter of $\Omega_{lum} \lesssim 0.01$. This information, combined with the fact that analysis of galactic rotational velocities implies >90% of the mass in galaxies is dark leads to the conclusion that $\Omega_{DM} \geq 0.09$. This is only a lower limit on the dark matter density parameter, since most rotation curves remain flat out to the largest radii at which they can be measured and it can be assumed that the DM halos extend even farther out.

With $\Omega_{DM} \geq 0.1$ it is possible that baryonic DM alone could be responsible for the dark matter halos. However, other analyses eliminate this possibility. Direct searches for massive compact halo objects (MACHOs) utilizing microlensing have determined that <25% of the dark halos could be due to baryonic dark matter within the mass range of $2 \times 10^{-7} M_{sun} < M < 1 M_{sun}$ at a 95% confidence limit [2, 3]. Furthermore, data from the Hubble Deep Field Space Telescope suggests dark matter halos consist of $\leq$5% white dwarfs.

With baryonic dark matter being ruled out as the sole component of dark mat-

ter halos we now investigate the other density parameter components. Big Bang nucleosynthesis models constrain the amount of baryonic matter in the universe to $\Omega_b \approx 0.045$ (where b stands for baryons) [28]. Additionally, analysis of velocity flows, x-ray emissions temperatures, and gravitational lensing in large clusters and superclusters of galaxies suggests that the total matter component of the universe has density parameter $\Omega_m \approx 0.2 - 0.3$. One can combine this information, assuming $h = 0.7$ to find density parameters that are consistent with the Planck observation of

$$\Omega_b = 4.9\%$$

$$\Omega_{nbm} = 26.8\%$$

$$\Omega_\Lambda = 68.3\%$$

where Ω_b is the baryonic density of the universe, Ω_{nbm} is the nonbaryonic density parameter of the universe, and Ω_Λ is the dark energy density parameter of the universe [27, 1]. This is known as the Λ-CDM model.

1.2.2 Nonbaryonic Dark Matter

With $\Omega_{nbm} = 26.8\%$ it is intriguing to look at the particles which have been proposed to explain this contribution to the total density parameter. One such particle is the standard-model neutrino. The neutrino is an electrically neutral, weakly interacting particle with a nearly zero mass. Neutrinos exist in three distinct flavors – the electron neutrino (ν_e), the muon neutrino (ν_μ), and the tau neutrino (ν_τ). It is known that neutrinos oscillate between these three flavors, with each flavor state being a super position of three neutrino states of definite mass (ν_1,ν_2, and ν_3). Ex-

periments studying solar neutrino oscillations have determined the squared mass difference between what is known as the solar neutrino doublet (ν_1 and ν_2) to be $\delta m^2 = (7.66 \pm 0.35) \times 10^{-5} eV^2$, while experiments studying atmospheric neutrino oscillations have determined the remaining squared mass difference between the solar neutrino doublet and ν_3 to be $\pm(2.38 \pm 0.27) \times 10^{-3} eV^2$ up to an unknown sign [25]. This sign ambiguity leads to two possible hierarchies for the neutrino mass states. (Figure 8) If we assume the normal hierarchy to be true, we can set a lower limit on the most massive neutrino state to be $m_{\nu_3} \gtrsim 0.05$ eV.

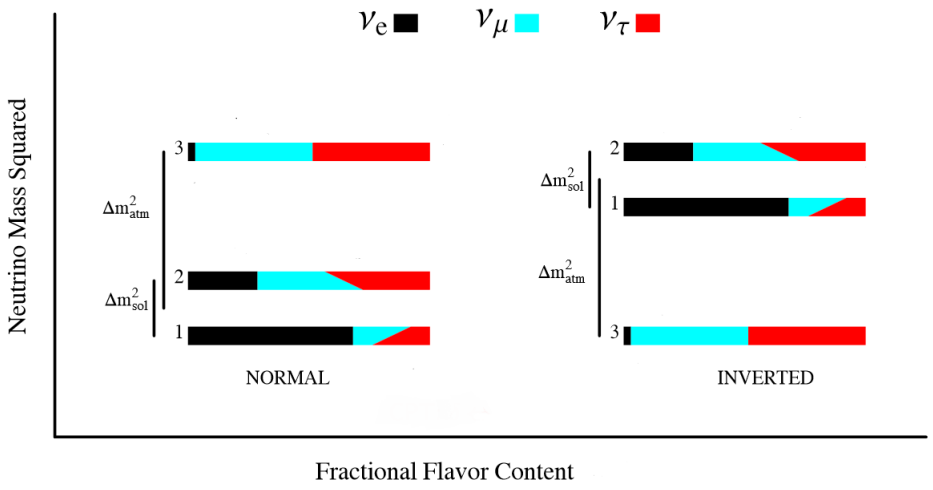

Figure 8: The two hierarchies of neutrino mass states. Black, teal, and red indicated the three flavors of neutrinos, while one, two, and three indicated the three mass states. [20]

The density parameter of neutrinos is given by

$$\Omega_\nu = \frac{\rho_\nu}{\rho_c} = \frac{1}{h^2} \sum_{i=1}^{3} \frac{g_i m_i}{90eV},$$

where $g_i = 1$ for Majorana neutrinos (own antiparticle) and $g_i = 2$ for Dirac neutrinos (distinct antiparticles) [21]. Using the lower mass limit of the neutrino

and assuming Majorana neutrinos, this suggests a lower limit on the neutrino density parameter of $\Omega_\nu \gtrsim 0.00122$. Thus, neutrinos do provide some contribution to the nonbaryonic dark matter density parameter.

To find an upper limit on the neutrino contribution to the nonbaryonic dark matter density parameter is is necessary to distinguish hot dark matter from cold dark matter. Hot dark matter is composed of particles that have zero or nearly-zero mass. Special relativity requires that the massless particles move at the speed of light, and that the nearly-massless particles move close to the speed of light. As a result hot dark matter forms very hot gases. Cold dark matter is composed of particles that have sufficient mass to travel at sub-relativistic velocities, thus forming colder gases. With their low masses neutrinos fall under the hot dark matter category. A combination of galaxy clustering measurements, CMB observations, and Lyman-α observations give an upper limit on the hot dark matter contribution of $\Omega_\nu \lesssim 0.0155$, thus neutrinos and other hot dark matter particles cannot be the primary contribution to the nonbaryonic dark matter density parameter [27].

1.2.3 WIMPs and SUSY

If we assume cold dark matter (CDM) particles were in thermal equilibrium with the other standard-model particles during the early stages (<1 ns) of the universe it is possible to calculate the CDM density parameter. According to Maxwell-Boltzmann statistics, as the temperature, T, of the universe cools, the particles with masses $m > T$ will diminish exponentially. Once the temperature of the universe cooled below the CDM mass scale the creation of these particles would have ceased. At this time the CDM particles which still existed would have continued annihilating with one another. As time went on, CDM annihilation became less

and less likely due to their dwindling abundance. Once the expansion rate of the universe, given by Hubble's constant, exceeded the CDM annihilation/creation rate, the CDM particles dropped out of thermal equilibrium and the CDM density became fixed.

The density parameter for CDM is approximately given by

$$\Omega_\chi h^2 \simeq \frac{T_0^3}{M_{Pl}\langle\sigma_A\nu\rangle}$$

where σ_A is the total annihilation cross section of CDM particles, ν is the relative velocity of CDM particles, T_0 is the equilibrium temperature, M_{Pl} is the Planck mass, c is the speed of light, and $\langle ...\rangle$ represents an average over the thermal distribution of CDM particle velocities [18, 17]. Remarkably, for the total density parameter of the universe to equal unity, as required by cosmological models, a cross section on the order of particles interacting on the electroweak scale ($\sim 10^{-9}GeV^{-2}$) is required for CDM particles. This result is the main motivation behind suspecting weakly interacting massive particles (WIMPs) as the dominant contribution to the nonbaryonic dark matter density parameter.

Supersymmetry (SUSY) is a symmetry of space-time which has been proposed in an effort to unify the electroweak, strong, and gravitional forces. This theory offers some insight into the nature of WIMPs. SUSY requires that a supersymmetric partner particle exists for each particle in the standard model. These partners go by the names of sleptons (partners of leptons), squarks (partners of quarks), gauginos (partners of gauge bosons), and higgsinos (partners of Higgs bosons). Sleptons and squarks have spin zero, while gauginos and higgsinos have spin one-half. Since none of these supersymmetric particles have been discovered it is thought they are

far more massive than their standard model counterparts, and thus that supersymmetry is not an explicit symmetry of nature.

Goldberg [14] and Ellis [13] have suggested that neutral gauginos and neutral higgsinos can mix together in a superposition known as the neutralino, χ. In most SUSY models, the neutralino is the lightest supersymmetric particle (LSP). In models which conserve R-parity (a new quantum number distinguishing SUSY particles from standard model particles) the LSP is stable, making it a prime candidate particle for dark matter. The expected cross section of neutralinos interacting via inelastic collisions with nucleons is dependent on the allowed regions of parameter space in the SUSY model being used. Results from the WMAP satellite refined this parameter space, concluding that the density parameter of neutralinos would be $0.192 < \Omega_\chi < 0.263$ [27, 7, 4].

The neutralino is one of many candidate particles suggested for WIMPs, and as previously mentioned, WIMPs are not the only candidate for dark matter. In the following sections we will briefly discuss some of the other candidates before returning to the discussion of WIMPs in Chapter **??**.

1.2.4 Axions and Axinos

Quantum chromodynamics (QCD) is a theory describing the strong interaction between quarks and gluons, which make up hadrons. In particle physics there exists a proposed symmetry of nature referred to as charge conjugation parity symmetry (CP-Symmetry). CP-Symmetry postulates that particles should behave the same if they are replace by their own antiparticle (C symmetry), and then have their parity reversed (P symmetry). Within QCD there is no theoretical reason to assume CP-symmetry exists. However, when a CP-violation term is included

in the QCD lagrangian its coefficient has been experimentally determined to be less than 10^{-10} [5]. This unexpected result is known as the strong CP problem in quantum chromodynamics. To reconcile this, a new symmetry known as the Peccei-Quinn theory has been proposed. This theory postulates the existence of a new pseudoscalar particle called the axion. According to the Peccei-Quinn theory, axions would be electrically neutral, low mass ($1\mu eV - 1eV$) particles that have very low interaction cross sections for the strong and weak forces. The axino arises when SUSY is introduced to the Peccei-Quinn theory, resulting in a supersymmetric partner to the axion known as the axino.

1.2.5 Gravitons and Gravitinos

In quantum field theory, the graviton is a hypothetical elementary particle which mediates the gravitational force. As with axions and axinos, when SUSY is introduced to quantum field theory a supersymmetric partner to the graviton is predicted to exist known as the gravitino. In some models, gravitinos are the LSP in SUSY and are thus a candidate particle for dark matter.

1.2.6 WIMPzillas

WIMPzillas are supermassive dark matter particles which arise when one considers the possibility that dark matter might be composed of nonthermal supermassive states. These particles would have a mass many orders of magnitude higher than the weak scale [10]. Studies have shown that for stable particles with masses close to $10^{13}\ GeV$ WIMPzillas would be produced in sufficient abundance to give $\Omega \approx 1$ for the total density parameter of the universe.

It should be noted that the discussion of this section does not encompass all

of the alternatives to WIMPs. Although these other dark matter candidates offer intriguing explanations to the dark matter problem, the next chapter will focus on the experimental detection of WIMPs.

References

[1] PAR Ade, N Aghanim, C Armitage-Caplan, M Arnaud, M Ashdown, F Atrio-Barandela, J Aumont, C Baccigalupi, Anthony J Banday, RB Barreiro, et al. Planck 2013 results. xv. cmb power spectra and likelihood. *Astronomy & Astrophysics*, 571:A15, 2014.

[2] C Afonso, JN Albert, J Andersen, R Ansari, É Aubourg, P Bareyre, JP Beaulieu, G Blanc, X Charlot, F Couchot, et al. Limits on galactic dark matter with 5 years of eros smc data. *Astronomy & Astrophysics*, 400(3):951–956, 2003.

[3] Charles Alcock, RA Allsman, David R Alves, TS Axelrod, Andrew C Becker, DP Bennett, Kem H Cook, N Dalal, Andrew John Drake, KC Freeman, et al. The macho project: microlensing results from 5.7 years of large magellanic cloud observations. *The Astrophysical Journal*, 542(1):281, 2000.

[4] Richard Arnowitt, Bhaskar Dutta, and Bo Hu. Dark matter, muon g-2 and other susy constraints. In *Beyond the Desert 2003*, pages 25–41. Springer, 2004.

[5] Varouzhan Baluni. Cp-nonconserving effects in quantum chromodynamics. *Physical Review D*, 19(7):2227, 1979.

[6] KG Begeman, AH Broeils, and RH Sanders. Extended rotation curves of spiral galaxies: Dark haloes and modified dynamics. *Monthly Notices of the Royal Astronomical Society*, 249(3):523–537, 1991.

[7] CL Bennett, M Halpern, G Hinshaw, N Jarosik, A Kogut, M Limon, SS Meyer, L Page, DN Spergel, GS Tucker, et al. First year wilkinson microwave anisotropy probe (wmap) observations: Preliminary maps and basic results. *The Astrophysical Journal Supplement Series*, 148(1):1, 2003.

[8] Amitai Yisrael Bin-Nun. Gravitational lensing with a large deflection angle as a probe of general relativity and the galactic center. *Publicly accessible Penn Dissertations*, 2010.

[9] Tremaine Binney. *Galactic Dynamics*. Princeton University Press, 2 edition, 2008.

[10] Daniel JH Chung, Edward W Kolb, and Antonio Riotto. Superheavy dark matter. *Physical Review D*, 59(2):023501, 1998.

[11] Douglas Clowe, Maruša Bradač, Anthony H Gonzalez, Maxim Markevitch, Scott W Randall, Christine Jones, and Dennis Zaritsky. A direct empirical proof of the existence of dark matter. *The Astrophysical Journal Letters*, 648(2):L109, 2006.

[12] Battaner E. and Florido E. The rotation curve of spiral galaxies and its cosmological implications. *Fund.Cosmic Phys.*, 21:1–154, 2000.

[13] John Ellis, John S Hagelin, Dimitri V Nanopoulos, K Olive, and Mark Srednicki. Supersymmetric relics from the big bang. *Nuclear Physics B*, 238(2):453–476, 1984.

[14] H Goldberg. Constraint on the photino mass from cosmology. *Physical Review Letters*, 50(19):1419, 1983.

[15] Wayne Hu. Cmb introduction. `http://background.uchicago.edu/~whu/intermediate/map1.html`, 2001. Accessed: 2016-06-14.

[16] D. Javorsek, II, E. Fischbach, and V. Teplitz. New Experimental Bounds on the Contributions to the Cosmological Density Parameter Ω from Strongly Interacting Massive Particles. *The Astrophysical Journal*, 568:1–8, March 2002.

[17] Gerard Jungman, Marc Kamionkowski, and Kim Griest. Supersymmetric dark matter. *Physics Reports*, 267(5):195–373, 1996.

[18] EW Kolb and MS Turner. The early universe, 1994.

[19] Hannu Kurki-Suonio. Lecture notes in cosmological perturbation theory. `http://theory.physics.helsinki.fi/~cpt/Cosmo12.pdf`, Fall 2015. Accessed: 2016-06-14.

[20] Stephen J. Parke. Determining the neutrino mass hierarchy. In *Third NO-VE International Workshop on Neutrino Oscillations in Venice : Fifty years after the neutrino esperimental discovery : Venezia, February 7-10, 2006, Istituto Veneto di Scienze, Lettere ed Arti, Campo Santo Stefano*, pages 115–125, 2006.

[21] Sergio Pastor. Light neutrinos in cosmology. *Physics of Particles and Nuclei*, 42(4):628–640, 2011.

[22] M. Persic, P. Salucci, and F. Stel. The universal rotation curve of spiral galaxies - I. The dark matter connection. *Monthly Notices of the Royal Astronomical Society*, 281:27–47, July 1996.

[23] S Pires, J-L Starck, and A Refregier. Light on dark matter with weak gravitational lensing. *arXiv preprint arXiv:0908.4157*, 2009.

[24] Alexandre Refregier. Weak gravitational lensing by large-scale structure. *Ann.Rev.Astron.Astrophys*, 41:645–668, 2003.

[25] RG Hamish Robertson. Direct determination of neutrino mass. In *Journal of Physics: Conference Series*, volume 173, page 012016. IOP Publishing, 2009.

[26] Barbara Sue Ryden. *Introduction to cosmology*, volume 4. Addison-Wesley San Francisco USA, 2003.

[27] David N Spergel, Licia Verde, Hiranya V Peiris, E Komatsu, MR Nolta, CL Bennett, M Halpern, G Hinshaw, N Jarosik, A Kogut, et al. First year wilkinson microwave anisotropy probe (wmap) observations: determination of cosmological parameters. *The Astrophysical Journal Supplement Series*, 148(1):175, 2003.

[28] David Tytler, David Kirkman, John M O'Meara, Nao Suzuki, Adam Orin, Dan Lubin, Pascal Paschos, Tridivesh Jena, Wen-Ching Lin, Michael L Norman, et al. Cosmological parameters sigma8, the baryon density, and the uv background intensity from a calibrated measurement of h i lyman-alpha absorption at z = 1.9. *The Astrophysical Journal*, 617(1):1, 2004.

[29] Jan van Paradijs and Johan AM Bleeker. X-ray spectroscopy in astrophysics. In *X-Ray Spectroscopy in Astrophysics*, volume 520, 1999.

[30] Alexey Vikhlinin, A Kravtsov, W Forman, C Jones, M Markevitch, SS Murray, and L Van Speybroeck. Chandra sample of nearby relaxed galaxy clusters: Mass, gas fraction, and mass-temperature relation. *The Astrophysical Journal*, 640(2):691–709, 2006.

[31] Xiang-Ping Wu, Tzihong Chiueh, Li-Zhi Fang, and Yan-Jie Xue. A comparison of different cluster mass estimates: consistency or discrepancy? *Monthly Notices of the Royal Astronomical Society*, 301(3):861–871, 1998.

[32] F. Zwicky. Republication of: The redshift of extragalactic nebulae. *General Relativity and Gravitation*, 41:207–224, January 2009.